

19 **1. Introduction**

20 The dramatic retreat of Arctic sea ice extent (SIE) during recent decades,
21 especially during summer [*Serreze et al.*, 2007; *Comiso et al.*, 2008] has been attributed
22 to changing patterns of surface winds [*Rigor et al.*, 2002; *Rigor and Wallace* 2004],
23 ocean currents [*Polyakov et al.*, 2005; *Shimada et al.*, 2006], and downward energy
24 fluxes from the atmosphere [*Francis and Hunter*, 2007; *Perovich et al.*, 2007].

25 In September 2007, Arctic sea-ice extent reached its lowest value since
26 microwave satellite measurements began in 1979. Most climate models have
27 underestimated the observed decline of Arctic SIE: the observed 2007 minimum was
28 much lower than simulated in any of the models participating in the Intergovernmental
29 Panel on Climate Change Fourth Assessment Report (IPCC AR4) [*Stroeve et al.*, 2007,
30 *Boe et al.* 2009]. The causes of the rapid decline in SIE remain uncertain.

31 Several recent studies have investigated the variations of Arctic sea ice extent
32 that occur in association with the dominant patterns of atmospheric circulation
33 variability. *Rigor et al.* [2002] suggested that the positive polarity of the wintertime
34 Arctic Oscillation (AO) induces negative anomalies in sea ice during the following
35 summer. *L'Heureux et al.*, [2008] suggested that the summertime Pacific-North
36 American (PNA) pattern has played a role in the rapid decline in summer SIE. The
37 so-called “winter dipole anomaly”, which corresponds to the second EOF of the sea

38 level pressure (SLP) field over the polar cap region, has been linked to the export of
39 Arctic sea ice [Wu *et al.*, 2006]. EOF-3 of the Northern Hemisphere SLP field has also
40 been mentioned in connection with the recent sea ice decline [Overland and Wang,
41 2005]. Ogi and Wallace [2007] have shown that years of low September SIE tend to be
42 characterized by anticyclonic summertime circulation anomalies over the Arctic Ocean.
43 The extreme loss of sea ice during summer 2007 was accompanied by strong anomalous
44 anticyclonic flow, with Ekman drift out of the marginal seas toward the central Arctic
45 [Ogi *et al.*, 2008]. Hence, there is evidence that both winter and summer atmospheric
46 circulation anomalies influence the extent of Arctic sea ice at the end of the summer
47 season.

48 In this study, we consider how the winds in the atmospheric boundary layer
49 force changes in September Arctic SIE from one year to the next and how they might
50 have contributed to the observed multidecadal decline in ice extent. In contrast to most
51 previous studies, we make use of estimated wind fields rather than estimated
52 geostrophic wind fields inferred from pressure fields and the domain in our study
53 extends beyond the Arctic Ocean to encompass the region of ice export through Fram
54 Strait and southward along the east coast of Greenland.

55

56 **2. Data and methods**

57 September SIE data from from 1979 to 2009 are based on *Comiso and Nishio*
58 [2008]. To represent the wind field, we use the National Centers for Environmental
59 Prediction/National Center for Atmospheric Research (NCEP/NCAR) reanalysis dataset
60 from 1979 to 2009 [Kistler *et al.*, 2001]. First, the 925-hPa wind fields are regressed on
61 September SIE to determine the seasonally-varying wind pattern that is linearly related
62 to the subsequent September SIE. The resulting regression maps are shown in the paper
63 and the corresponding correlation maps (not shown) are used as indicated below. Here,
64 “winter” is defined as JFMAM mean (the average for January through May). Similarly,
65 “summer” is defined as JJAS (the average for June through September).

66 Wind indices for each season in each calendar year are obtained by projecting
67 the JFMAM and JJAS wind fields for each year onto the corresponding correlation
68 patterns. We then use the time series of these winter and summer wind indices
69 time-series as predictors in a linear model to predict difference in September SIE from
70 one year to the next.

71

72

73

74 **3. Results**

75 Figure 1 shows the patterns of the winter and summer 925-hPa wind anomalies
76 regressed upon inverted one-year difference September SIE time series (Figs. 1a and
77 1b) and the inverted detrended September SIE time series (Figs. 1c and 1d) for the
78 period of record 1979-2009. Winter and summer linear trends as determined from a least
79 squares best fit regression are shown for comparison in Figs. 1e and 1f.

80 The 925-hPa wind anomalies in the winter preceding a low September SIE year
81 exhibit a strong northerly component to the north and east of Greenland in both for the
82 one-year difference data (Fig. 1a) and the detrended data (Fig. 1c). This pattern is
83 suggestive of an enhanced rate of flow of sea ice along the climatological-mean
84 wintertime ice edge from the Barents and Kara Seas and out through Fram Strait. Such a
85 transport would act to reduce the areal coverage of Arctic sea ice. Although the winter
86 trend pattern over the Arctic Ocean (Fig. 1e) is by no means identical to the regression
87 patterns (Figs. 1a and 1c), the features over the Barents Sea, Fram Strait and the
88 subpolar North Atlantic are remarkably similar; i.e., they are also suggestive of
89 enhanced forcing of sea ice transport toward and out through Fram Strait.

90 The patterns of summer winds regressed on one-year difference September SIE
91 (Fig. 1b) and detrended September SIE (Fig. 1d) are both characterized by anticyclonic

92 925-hPa wind anomalies over the Arctic Ocean. The anticyclonic flow is directed from
93 the Chukchi Sea across the Arctic Ocean toward Fram Strait, thus favoring enhanced sea
94 ice export into the Atlantic, as in winter, but with the ice coming from a different
95 direction. In summer, when the Arctic sea ice is thin and there are large expanses of
96 open water, the sea ice movement is close to free drift and hence the response of the sea
97 ice to the wind forcing may be larger than in winter. In the summer pattern associated
98 with the linear trend (Fig. 1f) the anticyclonic gyre is more restricted to the Beaufort Sea,
99 but it is also characterized by flow from the Chukchi Sea across the Arctic Ocean
100 toward Fram Strait. In all six panels of Fig. 1, the dominant feature in the wind field is
101 the anomalous northerly flow over and around Fram Strait.

102 Now we assess the influence of the winter and summer atmospheric
103 circulations on the changes in September Arctic SIE from one year to the next, making
104 use of regression analysis. We first generate winter and summer wind indices by
105 projecting the 925-hPa wind anomalies for each calendar year onto the correlation
106 patterns corresponding to the regression patterns shown in Fig. 1, weighting each grid
107 point in the summation by the area that it represents; i.e., by the cosine of its latitude.
108 The domain used in these projections is the oceanic region north of 65°N and is the
109 same one used in our previous studies [*Ogi and Wallace (2007), Ogi et al. (2008)*].

110 Time-series of the winter and summer indices obtained in this manner, with
111 reference to the change in September SIE from the preceding year to the current year,
112 are shown in Fig. 2a. The indices show positive trends of 0.252 standard deviation per
113 decade (winter) and 0.608/decade (summer) during the 30 year period of record
114 (1980-2009). The winter index increases occurred mainly during the first half of the
115 record, while the increases in summer index occurred later in the record.

116 In 2007 when the record-low minimum in September SIE was observed, the
117 summer index exhibited a record high positive value and the winter index a moderately
118 high positive value. In contrast, in 1996 when the record-high maximum was observed,
119 both winter and summer indices exhibited near-record low negative values.

120 Using the two wind indices shown in Fig. 2a, the one-year change in
121 September SIE is predicted by a multiple regression model with cross validation,
122 withholding one year at a time in making regression model and predicting the one-year
123 change in September SIE for the withheld year. Results are shown in Figure 2b; the
124 correlation coefficient is 0.71. The regression coefficients for winter and summer winds
125 are -0.585 and -0.244 , respectively. The prediction scheme based on the cross validated
126 results is statistically significant at the 99.9% level and accounts for 50% of the variance
127 of the September SIE time series.

128 Having shown that winter and summer wind forcing influence September SIE,
129 we will now take into account the preconditioning of the sea by introducing into the
130 regression model the data for September SIE for the previous year. Figure 2c shows the
131 time series of observed and predicted current September SIE based on cross-validated
132 data, using as linear predictors the winter and summer indices shown in Fig. 2a together
133 with the observed SIE for the previous September. The results prove to be a good
134 prediction of September SIE (cross-validated $R=0.91$). The regression coefficients
135 without cross validation for previous September SIE, the winter winds and the summer
136 winds are 0.593, -0.510 and -0.325, respectively. Considering that September SIE for
137 the previous year is one of the predictors, the fact that the prediction replicates the
138 downward trend in Sep SIE is in no way remarkable and does not prove that the trends
139 in the wind indices in Fig. 2a are responsible for it.

140 *Ogi et al* 2008 used a summer sea level pressure index as the sole indicator of
141 atmospheric conditions and they used the areal coverage of multi-year ice in May to
142 represent the preconditioning of the ice. The correlation coefficient of the predicted
143 September SIE based on the previous September SIE, the winter wind and the summer
144 wind indices shown in Fig. 2c has proven to be higher than that obtained by *Ogi et al.*
145 2008 ($R = 0.91$ versus $R = 0.82$). This result suggests that the wind anomalies in both

146 the previous winter and the previous summer influence September SIE and that the flow
147 of ice from Arctic Ocean toward Fram Strait, which was not specifically considered in
148 our previous study, plays a key role. The higher correlation could also indicate that
149 wind patterns are better predictors of September SIE than sea-level pressure patterns.

150 We repeat the above analysis using the correlation patterns and indices based
151 on detrended data (Figs. 1c and 1d) in place of the one-year difference data. In this case
152 only the winter and summer wind indices are used as predictors, but in deriving the
153 indices we project the total wind anomalies, including trends, onto the correlation
154 patterns. A similar methodology was used by *Thompson et al.* (2000). The winter and
155 summer indices show positive trends from 1979 to 2009 (0.339 and 0.387 per decade,
156 respectively). Then, the September SIE is predicted using these two indices (Fig. 3b).
157 The correlation coefficient with validation is 0.74, and the trends in observed and
158 predicted September SIE are -0.779 and -0.266 per decade, respectively. Hence, it
159 appears that about one-third of observed trend of September SIE is explained by the
160 wind forcing alone.

161 Both winter and summer winds are important for September SIE. However, it
162 is notable that recent large losses of September sea ice in 2005, 2007 and 2008 could
163 not have been well predicted without including the summer index.

164 **4. Conclusions and discussion**

165 We have shown results indicating that wind-induced, year-to-year differences
166 in the rate of flow of ice toward and through Fram Strait play an important role in
167 modulating September sea-ice extent on a year-to-year basis and that a trend toward an
168 increased rate of flow has contributed to the decline in the areal coverage of Arctic
169 summer sea ice.

170 *Kwok* [2009] examined year-to-year variability and trends in ice outflow into
171 the Greenland and Barents Seas for the period 1979-2007 on the basis of passive
172 microwave brightness temperature and ice concentration and SLP data. He also found
173 evidence of increased wind forcing of ice export through Fram Strait but in his analysis
174 the increased rate of flow was accompanied by a trend toward decreased sea ice
175 concentrations in this region, so that the actual export of ice through Fram Strait showed
176 little, if any long term trend over the 29-year period of record. However, he reported a
177 systematic increase in the flux of ice toward Fram Strait in the trans-polar drift,
178 particularly during summer, consistent with the wind pattern in our Fig. 1f. Our results
179 also serve to confirm recent findings of *Ogi and Wallace* [2007] and *Ogi et al.* [2008]
180 that anticyclonic circulation anomalies over the Arctic during summertime favor low
181 sea-ice extent and that the winds over the Arctic Ocean have exhibited a trend in this

182 sense, especially during the past decade.

183 It is notable that the wind and patterns obtained in this study and the SLP
184 patterns implied by them do not correspond to the teleconnection patterns emphasized
185 in previous studies— i.e., the AO [*Rigor et al.*, 2002], the PNA pattern [*L'Heureux et al.*,
186 2008] and the Dipole Anomaly pattern [*Wu et al.*, 2006] — quite possibly because the
187 methodology used in our study is different. In the studies cited above the dominant
188 spatial pattern of atmospheric variability pattern was obtained by EOF analysis and the
189 expansion coefficient (or principal component) time series of that pattern was correlated
190 with the time series of sea ice extent. In contrast, the patterns identified in this study are
191 obtained by direct linear regression of the 925 hPa wind field on time series of sea ice
192 extent. These regression patterns have significant onto the EOFs of the SLP field (e.g.,
193 the summer pattern resembles the summer Northern Hemisphere annular mode
194 described by *Ogi et al.*, 2004 to some extent) but the correspondence is not perfect.

195 We repeated the analysis keeping everything the same, but using the SLP field
196 instead of 925-hPa wind field. The SLP patterns (not shown) are consistent with the 925
197 hPa wind patterns in Fig. 1 and time-varying indices derived from them (not shown) are
198 very similar to those shown in Fig. 2a. However, it is notable that the correlations
199 between the predicted and observed time series of September SIE are higher for the

200 predictors based on wind data: $R = 0.71$ for wind versus 0.64 for SLP for the predicted
201 and observed time series in Fig. 2b, 0.91 versus 0.85 for those in Fig. 2c, and 0.74
202 versus 0.49 for those shown in Fig. 3b. The statistical correlations between SIE and
203 wind are higher than those between SIE and SLP because the physical relationship is
204 more direct.

205 The diagnostics used in this study may be useful for describing and comparing
206 how the sea ice fields in sea climate models respond to the variations in the wind field.
207 It would also be of interest to make a more direct comparison between the wind fields
208 examined in this study and the two-dimensional field of satellite-derived ice-area flux
209 examined in the study of *Kwok* [2009].

210

211 **Acknowledgments**

212 We thank I. Rigor for providing the September SIE data. J.M. Wallace was supported by
213 the Climate Dynamics Program of the U.S. National Science Foundation under Grant
214 GA 0812802

215

216 **References**

217 Boe J., A. Hall, and X. Qu (2009), September sea-ice cover in the Arctic Ocean

218 projected to vanish by 2100. *Nature Geoscience*, doi:10.1038/NGEO467.

219 Comiso, J. C., and F. Nishio (2008), Trends in the sea ice cover using enhanced and
220 compatible AMSR-E, SSM/I, and SMMR data. *J. Geophys. Res.*, 113, C02S07,
221 doi:10.1029/2007JC004257.

222 Comiso, J. C., C. L. Parkinson, R. Gersten, and L. Stock (2008), Accelerated decline in
223 the Arctic sea ice cover, *Geophys. Res. Lett.*, 35, L01703,
224 doi:10.1029/2007GL031972.

225 Francis, J. A., and E. Hunter (2007), Drivers of declining sea ice in the Arctic winter: A
226 tale of two seas, *Geophys. Res. Lett.*, 34, L17503, doi:10.1029/2007GL030995.

227 Kistler R, E. Kalnay, and co-authors (2001), The NCEP-NCAR 50-year reanalysis:
228 Monthly means CD-ROM and documentation. *Bull. Amer. Meteor. Soc.*, 82(2),
229 247-267.

230 Kwok, R. (2009), Outflow of Arctic ocean sea ice into the Greenland and Barents seas:
231 1979-2007, *J. Clim.*, 22, 2438-2457.

232 L'Heureux, M. L., A. Kumar, G. D. Bell, M. S. Halpert, and R. W. Higgins (2008), Role
233 of the Pacific-North American (PNA) pattern in the 2007 Arctic sea ice decline,
234 *Geophys. Res. Lett.*, 35, L20701, doi:10.1029/2008GL035205.

235 Ogi, M., K. Yamazaki, and Y. Tachibana (2004), The summertime annular mode in the

236 northern hemisphere and its linkage to the winter mode, *J. Geophys. Res.*, 109,
237 D20114, doi:10.1029/2004JD004514.

238 Ogi, M., and Wallace, J. M. (2007), Summer minimum Arctic sea ice extent and
239 associated summer circulation. *Geophys. Res. Lett.*, 34, L12705,
240 doi:10.1029/2007GL029897.

241 Ogi, M., I. G. Rigor, M. G. McPhee, and J. M. Wallace (2008), Summer retreat of Arctic
242 sea ice: Role of summer winds, *Geophys. Res. Lett.*, 35, L24701,
243 doi:10.1029/2008GL035672.

244 Overland, J. E., and M. Wang, The third Arctic climate pattern: 1930s and early 2000s
245 (2005), *Geophys. Res. Lett.*, 32, L23808, doi:10.1029/2005GL024254.

246 Perovich, D. K., B. Light, H. Eicken, K. F. Jones, K. Runciman, and S. V. Nghiem
247 (2007), Increasing solar heating of the Arctic Ocean and adjacent seas, 1979-2005:
248 Attribution and role in the ice-albedo feedback, *Geophys. Res. Lett.*, 34, L19505,
249 doi:10.1029/2007GL031480.

250 Polyakov, I. V. and 22 co-authors (2005), One more step toward a warmer Arctic,
251 *Geophys. Res. Lett.*, 32, L17605, doi:101029/2005GL023740.

252 Rigor, I. G., J. M. Wallace, and R. L. Colony (2002), Response of sea ice to the Arctic
253 Oscillation, *J. Clim.*, 15, 2648-2663.

254 Rigor, I. G. and J. M. Wallace (2004), Variations in the age of Arctic sea-ice and summer
255 sea-ice extent, *Geophys. Res. Lett.*, 31, L09401, doi:10.1029/2004GL019492.

256 Serreze, M. C., M. M. Holland, and J. K. Stroeve (2007), Perspectives on the Arctic's
257 shrinking sea-ice cover, *Science*, 315, 1533-1536.

258 Shimada, K., T. Kamoshida, M. Itoh, S. Nishio, E. Carmack, F. McLaughlin, S.
259 Zimmermann, and A. Proshutinsky (2006), Pacific Ocean inflow: Influence on
260 catastrophic reduction of sea ice cover in the Arctic Ocean. *Geophys. Res. Lett.*, 33,
261 L08605, doi:10.1029/2005GL025624.

262 Stroeve, J., M. M. Holland, W. Meier, T. Scambos, and M. Serreze (2007), Arctic sea ice
263 decline: Faster than forecast. *Geophys. Res. Lett.*, 33, L09501,
264 doi:10.1029/2007GL029703.

265 Thompson, D. W. J., J. M. Wallace, and G. C. Hegerl (2000), Annular modes in the
266 extratropical circulation. Part II. Trends, *J. Clim.*, 13, 1018-1036.

267 Wu, B., J. Wang, and J. E. Walsh (2006), Dipole anomaly in the winter Arctic
268 atmosphere and its association with sea ice motion, *J. Clim.*, 19, 210-225.

269
270

271 **Figure Captions**

272 Figure 1: (a) Wind at 925 hPa in winter (JFMAM) regressed on the inverted one-year

273 difference of September Arctic SIE for the period 1979-2009. (b) As in Figure 1a, but in
274 summer (JJAS) (c) Detrended wind at 925 hPa in winter regressed on the time series of
275 inverted, detrended September SIE. (d) As in Figure 1c, but for summer. (e) The linear
276 trend of 925-hPa winter wind (per decade) (f) As in Figure 1e, but for summer wind.

277

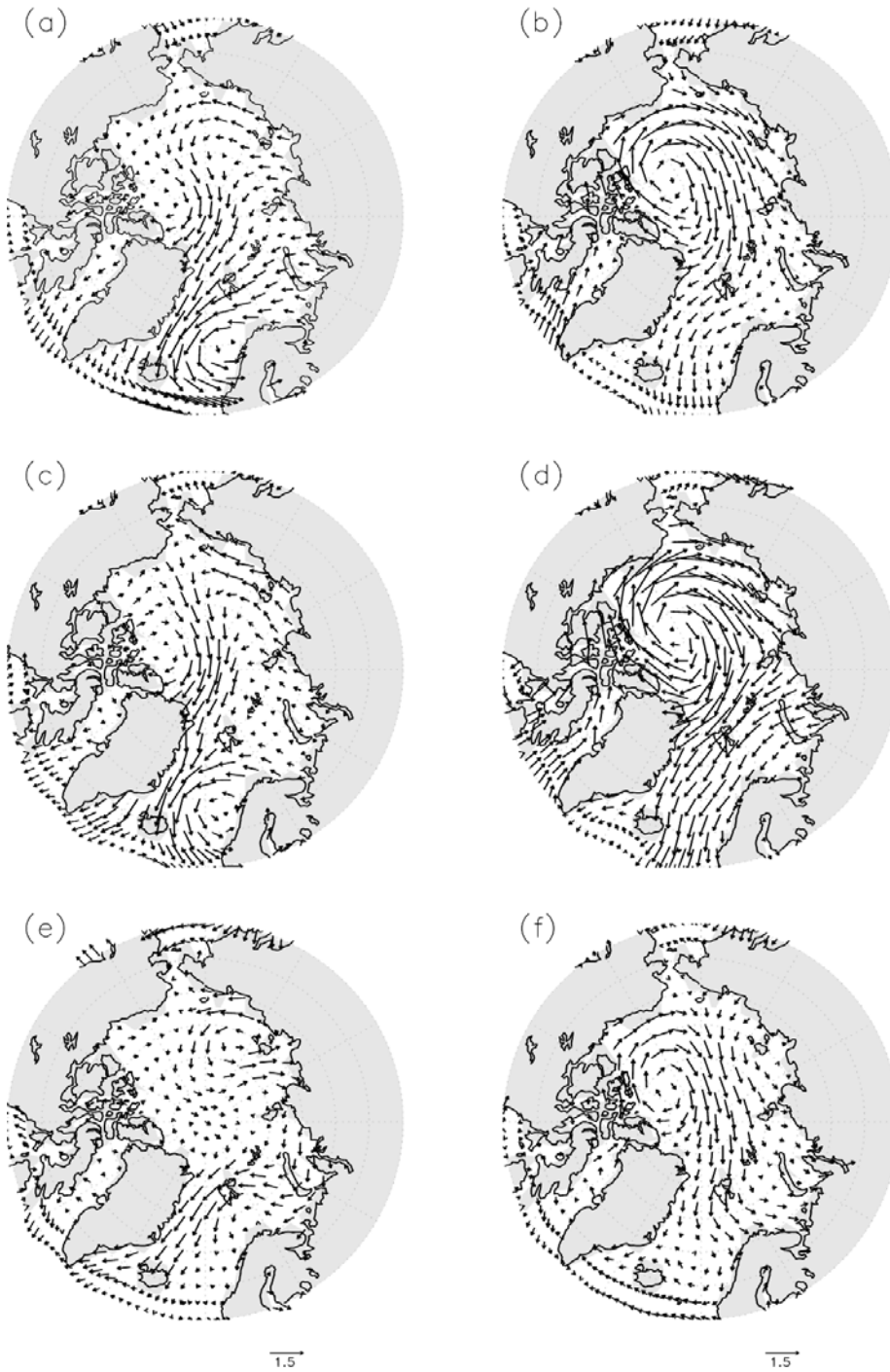
278 Figure 2: (a) Time-series of standardized winter (white) and summer (black) indices
279 based on 925-hPa correlation patterns obtained by regressing JFMAM-mean wind fields
280 for each year upon the one-year difference of September SIE from the previous year to
281 the current year. The corresponding regression patterns are shown in Figure 1a and 1b.
282 (b) Observed (black circles) and predicted (open squares) one-year difference of
283 September SIE using a prediction model with winter and summer wind indices in Fig.
284 2a as predictors, with cross validation ($R=0.71$) (c) As in (b) but including, as a third
285 predictor, the previous September SIE ($R=0.91$).

286

287 Figure 3: (a) As in Figure 2a but using detrended 925-hPa wind patterns regressed on
288 detrended September SIE, shown in Figure 1c and 1d. (b) Observed (black circles) and
289 predicted (open squares) September SIE prediction model based on cross validated
290 dataset using winter and summer indices shown Figure 3a ($R=0.74$).

291

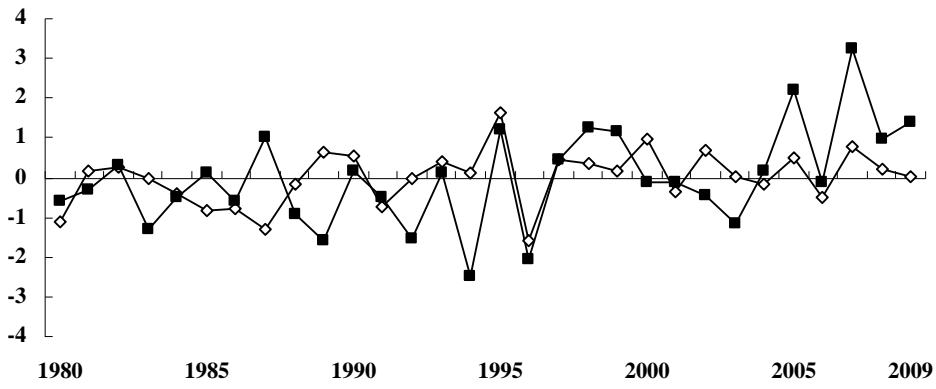
292
293
294



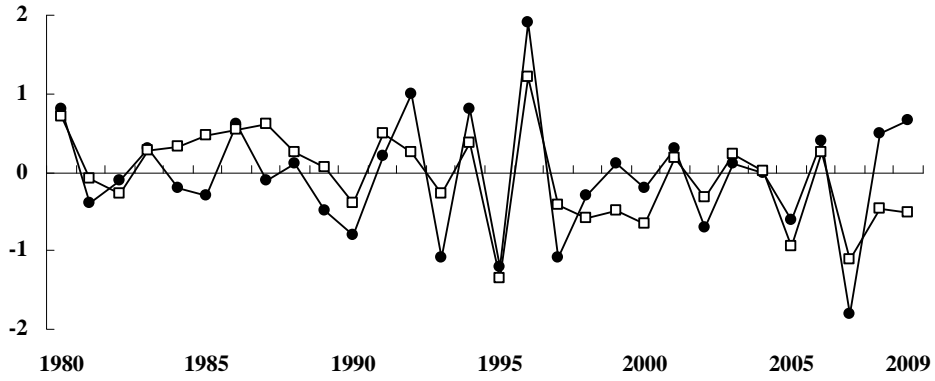
295
296
297

Figure 1

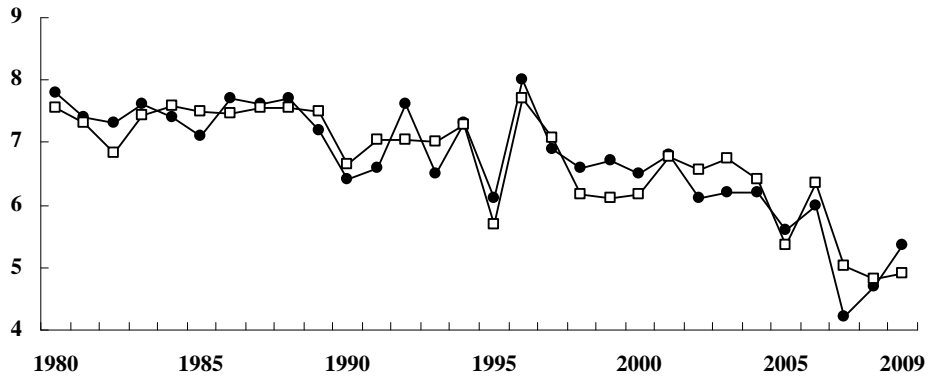
298
299



300



301



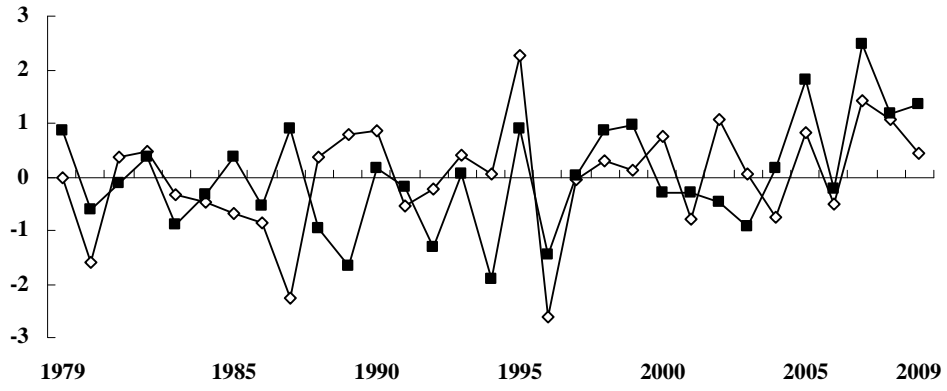
302

303

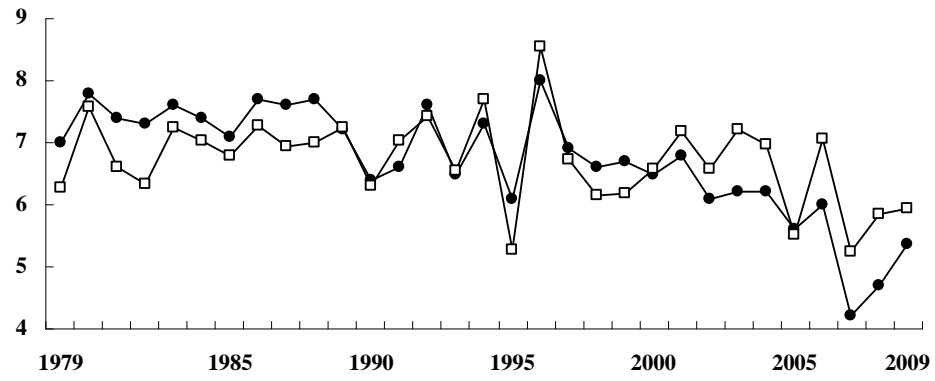
304

Figure 2

305
306
307



308



309
310
311
312

Figure 3